

Study of the neutron-rich region in the vicinity of ^{208}Pb via multinucleon transfer reactions

Petra Čolović^{1,*}, Andrés Illana², Suzana Szilner¹, Jose-Javier Valiente-Dobón², Lorenzo Corradi², Tea Mijatović¹, Giovanna Benzoni³, María José García Borge⁴, Alberto Boso⁵, Simone Ceruti³, James Cubiss⁶, Giacomo de Angelis², Enrico Fioretto², Franco Galtarossa², Liam Paul Gaffney⁷, Maria de La Luz Jurado-Gomez⁸, Thorsten Kröll⁹, Tommaso Marchi², Roberto Menegazzo⁴, Daniele Mengoni⁴, Daniel R. Napoli², Zsolt Podolyak¹⁰, Giovanni Pollarolo¹¹, Francesco Recchia⁴ and Dmitry Testov⁴

¹Ruder Bošković Institute, Zagreb, Croatia

²Istituto Nazionale di Fisica Nucleare (INFN), Laboratori Nazionali di Legnaro, Legnaro, Italy

³Dipartimento di Fisica, Università di Milano and INFN, Milano, Italy.

⁴Instituto de Estructura de la Materia CSIC, Madrid, Spain

⁵Dipartimento di Fisica e Astronomia, Università di Padova, and INFN, Padova, Italy

⁶Department of Physics, University of York, York, United Kingdom

⁷ISOLDE, CERN, Geneva, Switzerland

⁸Instituto de Física Corpuscular CSIC, Valencia, Spain

⁹Institut für Kernphysik, Technische Universität Darmstadt, Darmstadt, Germany

¹⁰University of Surrey, Guildford, United Kingdom

¹¹Dipartimento di Fisica, Università di Torino and INFN, Torino, Italy

Abstract. The multinucleon transfer reaction mechanism was employed to populate isotopes around the doubly-magic ^{208}Pb nucleus. We used an unstable ^{94}Rb beam on ^{208}Pb targets of different thickness. Transfer channels were studied via the fragment- γ and γ - γ coincidences, by using MINIBALL γ spectrometer coupled to a particle detector. Gamma transitions associated to the different Pb isotopes, populated by the neutron transfers, are discussed in terms of excitation energy and spin. Fragment angular distributions were extracted, and compared with the reaction models.

1 Towards the neutron-rich heavy nuclei

The study of heavy neutron-rich nuclei in the vicinity of the $N = 126$ shell closure is nowadays in the focus of nuclear physics. The properties of these nuclei are crucial to understand the synthesis of heavy elements. At the same time, this region of the nuclear chart is difficult to access experimentally.

One of the promising tools to reach this heavy neutron-rich region of the nuclear chart is the transfer of many nucleons at energies close to the Coulomb barrier. In fact, in the last decade, the multinucleon transfer (MNT) reactions [1, 2] were extensively used to populate moderately neutron-rich nuclei. Combining the stable (medium-heavy) projectile onto a (heavy) target results in nucleon transfers, with the cross section of each transfer channel governed by optimum Q -value considerations and nuclear form factors. Recently, the total cross sections of different transfer channels were compared for several systems having the same ^{208}Pb target and with projectiles going from neutron-poor to neutron-rich nuclei, i.e., ^{40}Ca , ^{58}Ni , and ^{40}Ar [3]. The neutron-rich (stable) ^{40}Ar beam allowed to get access to the channels involving proton pick-up, lead-

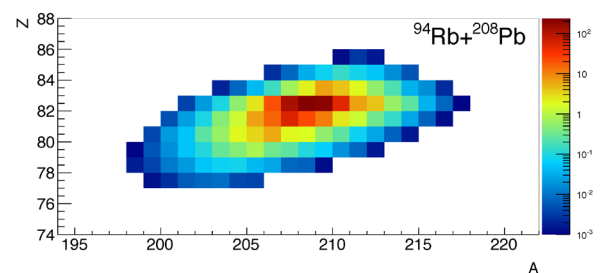


Figure 1. The $^{94}\text{Rb}+^{208}\text{Pb}$ reaction cross section distribution [mb] for the heavy partner calculated by the GRAZING code at $E_{\text{lab}}(^{94}\text{Rb}) = 583$ MeV. The calculated cross section includes the effect of neutron evaporation.

ing to the neutron-rich heavy partner. These data were compared with the GRAZING code [4–6]. GRAZING calculates the evolution of the reaction by taking into account, besides the relative motion variables, the intrinsic degrees of freedom of projectile and target, the surface modes and the one-nucleon transfer channels. The relative motion of the system is calculated in a nuclear plus Coulomb field.

*e-mail: petra.colovic@irb.hr

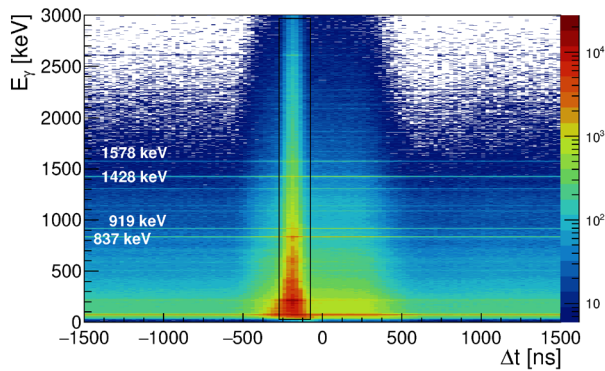


Figure 2. Gamma energy (E_γ) vs. the time difference (Δt) between the particle and γ . The 13 mg/cm^2 ^{208}Pb target was used. The prompt particle- γ coincidences are contained inside the gate of the $\Delta t = 200 \text{ ns}$ width. Left from the prompt peak is the isomeric part of the spectrum (delayed region). The strongest background lines are labeled.

The exchange of many nucleons proceeds via a multi-step mechanism of single nucleons.

The same model predicts that by using the (very) neutron-rich unstable beams, the proton pick-up and neutron stripping channels become the dominant ones [7]. Other reactions models, envisaging different mechanisms for the production of heavy neutron-rich nuclei [8, 9], reach the similar conclusions. It was also emphasized that secondary processes, like for example neutron evaporation, may significantly influence the final yield distributions. How to successfully transfer neutrons to the heavy target, while minimizing the influence of the secondary processes, is still an open question (see for example Ref. [10, 11] and references therein).

In order to explore the favorable experimental conditions for the population of the heavy neutron-rich nuclei by the MNT, we performed the measurement of a $^{94}\text{Rb}+^{208}\text{Pb}$ reaction at energy close to the Coulomb barrier. This relatively intense neutron-rich beam in the mass region $A \sim 95$ has been used, in order to achieve a transfer yield sufficient for the detection, while taking into account also the predicted cross section for the population of the southwest region of the nuclear chart around ^{208}Pb . The prediction of the cross section distribution by the GRAZING code is plotted in Fig. 1. As expected, the largest calculated cross sections are in the neutron transfer channels, being the cross section of the ^{209}Pb larger than the ^{207}Pb one. In this work we will present details of the experimental method and some selected results, concentrating on the neutron transfer channels.

2 The $^{94}\text{Rb}+^{208}\text{Pb}$ experiment

The ^{94}Rb radioactive ion beam at $E_{\text{lab}} = 6.2 \text{ MeV}\cdot A$ was delivered by the HIE-ISOLDE facility in CERN onto ^{208}Pb targets of different thickness. Experimental set-up consisted of the MINIBALL γ -array coupled to the Compact-Disk (CD) particle detector. MINIBALL consists of the

24 high-purity germanium crystals, individually encapsulated in triple-cluster cryostats which surround the spherical target chamber in compact geometry [12]. The absolute efficiency of 8% (at 1.3 MeV) is obtained, with the position sensitivity being preserved via six-fold electrical segmentation of the each crystal electrode. Four Double-sided Silicon Strip Detectors (DSSSD) were arranged in the CD configuration, positioned 21 mm downstream of the target with respect to the incoming beam. Front side of each DSSSD is made of 16 annular strips spanning a $24^\circ - 63^\circ$ angular range.

The identification of reaction products was obtained via their associated γ rays. Fragment- γ coincidences are illustrated in Fig. 2, where the energy, E_γ , is plotted as a function of the time difference between the detected particle and a γ -ray. The same figure also shows how the prompt coincidences (within $\Delta t = 200 \text{ ns}$) can be separated from the isomeric contribution (on the left side of the prompt region). The spectrum at the right side of the prompt peak illustrates well the complex background. The strongest γ rays, coming from the ^{94}Rb beta-decay chain, were attributed to the ^{94}Sr (837 and 1578 keV lines), ^{94}Y (1428 keV line) and ^{94}Zr (919 keV line). The ^{94}Sr was present also as the beam impurity (10% of the total flux). The background was successfully reduced by subtraction of the random particle- γ coincidences from the prompt and delayed events.

The ^{208}Pb targets of two different thickness were employed, 1 mg/cm^2 and 13 mg/cm^2 . We used the thin, 1 mg/cm^2 target, to extract quantitative information relevant for the reaction mechanism, like the angular distributions of different channels. Gamma rays were emitted in flight, thus the Doppler corrections had to be applied for the both Rb-like and Pb-like fragments. The selection of the fragment in the CD detector improved Doppler correction, and the resolution of 1.2% at 1.5 MeV was obtained. These Doppler corrected spectra, for the Rb-like and Pb-like fragments, are plotted in Fig. 3, for a selected energy range. An additional gate was applied to select a prompt coincidence with the Rb-like fragments, and it enabled to obtain a cleaner spectra. In the case of the ^{208}Pb 13 mg/cm^2 thick target, where the Pb-like fragments were stopped, we studied the structure of the strongly populated states via γ - γ coincidences.

3 Results and discussion

The matrix of the fragment energy plotted as a function of the scattering angle, detected with the CD detector, is shown in the Fig. 4. A clear separation of the Rb-like and Pb-like fragments is visible. From this $E - \theta$ matrix we extracted the angular distributions for the total quasi-elastic scattering of the detected Rb-like and Pb-like fragments, and combined them in a single distribution. We remind that we do not have charge and mass identification in the CD detector, thus the experimental distribution, especially around the grazing angle, is a sum of the elastic, inelastic and transfer differential cross sections. Such distribution is a pure Rutherford scattering at the most forward measured angles, which was used to obtain a normalization factor.

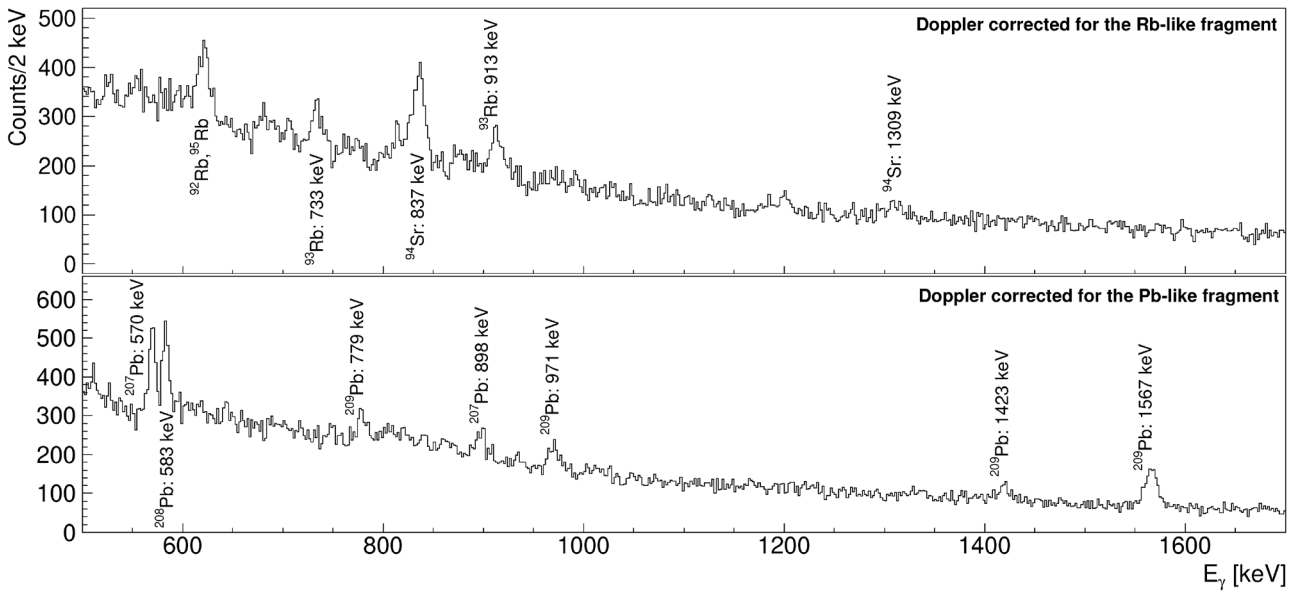


Figure 3. Gamma-spectra Doppler corrected for the Rb-like ($\beta \sim 10\%$), and Pb-like fragments ($\beta \sim 3\%$), is shown on the top, and bottom, respectively. The strongest γ -transitions within a selected energy range are labeled. For the Pb isotopes they correspond to the following transitions: ^{207}Pb , $E_\gamma = 570$ keV ($5/2^- \rightarrow 1/2^-$) and 898 keV ($3/2^- \rightarrow 1/2^-$), ^{208}Pb , $E_\gamma = 583$ keV ($5^- \rightarrow 3^-$), ^{209}Pb , $E_\gamma = 779$ keV ($11/2^+ \rightarrow 9/2^+$), $E_\gamma = 971$ keV ($3/2^+ \rightarrow 5/2^+$), $E_\gamma = 1423$ keV ($15/2^- \rightarrow 9/2^+$), $E_\gamma = 1567$ keV ($5/2^+ \rightarrow 9/2^+$).

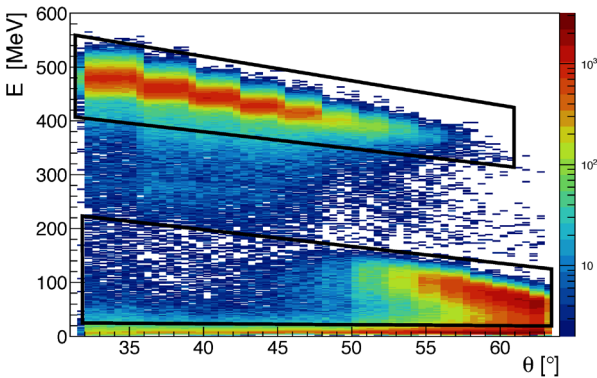


Figure 4. Two-dimensional matrix of angle (θ) vs. the energy (E) measured with the CD detector for the $^{94}\text{Rb}+^{208}\text{Pb}$ reaction. The Rb-like (top) and Pb-like (bottom) reaction products are labeled.

The results have been compared with the GRAZING calculations for the entrance channel mass partition. It was found that the measured and calculated differential cross sections agree well at the forward angle and at the quarter point.

In a similar way, by using the fragments in prompt coincidence with γ rays, we constructed angular distributions of strongly excited states, in particular of the 3^- state at 2614.5 keV in ^{208}Pb . The comparison of the obtained distribution with the reaction models, for example, distorted-wave Born approximation calculation, will provide (besides the normalization factor) the interaction potential and will better define the degrees of freedom which are important in the reaction.

In the reaction models the excitation and transfer processes are mediated by the well known single-particle form factors for the fermion degrees of freedom and by the collective form factors, for the vibrational modes. The same degrees of freedom should play a significant role in the distribution of the transfer strength over different states. Preliminary identification of $^{207,208,209}\text{Pb}$ transitions indicates the selective population of excited states (see Fig. 3). In ^{208}Pb the strongest observed transition is the $3^- \rightarrow 0^+$, $E_\gamma = 2614.5$ keV. In one-neutron transfer channels, ^{207}Pb and ^{209}Pb , we observed a significant population of the states of single-particle character. Besides the single-particle character, we also observed the population of the states with the main configuration which can be described as a coupling of the valence neutron (hole) to the ^{208}Pb octupole. The same phenomena, the strong population of the stretched configuration of particle-phonon states, was previously observed in different measured systems [13–16] by using MNT reactions. In neutron transfer channels we measured excitation energies up to ~ 4 MeV and up to relatively high-spin (i.e. up to $\sim 12\hbar$ in ^{209}Pb). In the ^{210}Pb , a decay chain from 10^+ to 0^+ was observed, by using the 13 mg/cm² thick target and by combining the prompt and delayed transitions in γ - γ coincident analysis. This allowed to measure the decay of the 6^+ and 8^+ isomeric states as well.

Recently, the level scheme of the ^{210}Pb nuclei, populated in the $^{208}\text{Pb}+^{208}\text{Pb}$ transfer and deep-inelastic reactions, was established on the basis of prompt and delayed γ - γ coincidences [17], adding previously unobserved states. The neutron rich Pb isotopes were populated by using the fragmentation of the ^{238}U beam [18]. In this measurement, the neutron-rich lead isotopes up to ^{216}Pb were studied by the isomeric-decay γ spectroscopy.

The obtained results were compared with the state-of-the-art shell-model calculations and discussed in terms of the effective three-body interactions and two-body transition operators. These two recent works demonstrate the complementarity of the reaction mechanisms.

4 Summary

We measured the $^{94}\text{Rb}+^{208}\text{Pb}$ transfer reaction, by using the neutron-rich unstable beam of the ISOLDE facility. The high-resolution MINIBALL spectrometer, coupled to a position sensitive silicon CD detector, allowed the identification of reaction products via their associated γ rays. The multinucleon transfer reactions were proposed as an efficient reaction mechanism for the production of the moderately neutron-rich nuclei in the vicinity of ^{208}Pb . As we observed a larger cross section in ^{209}Pb than in ^{207}Pb , these preliminary findings indicate that the used mechanism is a very promising tool for studies of the hard-to-reach neutron-rich isotopes around the ^{208}Pb . The more detailed study of the distribution of the transfer strength over different states will shed a light on important degrees of freedom which influence the evolution of reaction.

Acknowledgments

The authors are grateful to the INFN - LNL target laboratory for the excellent targets. This work was partly supported by the HORIZON2020 ENSAR2 Grant Agreement nb. 654002. This work has been supported in part by the

Croatian Science Foundation under project no. 7194 and in part under project no.IP-2018-01-1257.

References

- [1] L. Corradi, G. Pollarolo, and S. Szilner, *J. of Phys. G* **36**, 113101 (2009)
- [2] R. Broda, *J. of Phys. G* **32**, R151 (2006)
- [3] T. Mijatović et al, *Phys. Rev. C* **94**, 064616 (2016)
- [4] A. Winther, *Nucl. Phys. A* **572**, 191 (1994)
- [5] A. Winther, *Nucl. Phys. A* **594**, 203 (1995)
- [6] Program GRAZING <http://www.to.infn.it/nanni/grazing>
- [7] C. H. Dasso, G. Pollarolo, and A. Winther, *Phys. Rev. Lett.* **73**, 1907 (1994)
- [8] V. I. Zagrebaev and W. Greiner. *Phys. Rev. C* **83**, 044618 (2011)
- [9] L. Zhu et al., *Phys.Lett. B* **767**, 437 (2017)
- [10] F. Galtarossa et al, *Phys. Rev. C* **97**, 054606 (2018)
- [11] Y. X. Watanabe, *Phys. Rev. Lett* **115**, 172503 (2015)
- [12] N. Warr et al., *Eur. Phys. J. A* **49**, 40 (2013)
- [13] S. Lunardi et al., *Phys. Rev. C* **76**, 034303 (2007)
- [14] S. Szilner et al., *Phys. Rev. C* **84**, 014325 (2011)
- [15] D. Montanari et al., *Phys.Lett. B* **697**, 288 (2011)
- [16] P. Čolović et al., *Eur. Phys. J. A* **53**, 8 (2017)
- [17] R. Broda et al, *Phys. Rev. C* **98**, 024324 (2018)
- [18] A. Gottardo et al., *Phys. Rev. Lett.* **109**, 162502 (2012)